Deep-dwelling foraminifera as thermocline temperature recorders

Caroline Cléroux, Elsa Cortijo, Jean-Claude Duplessy, Rainer Zahn

Geochemistry Geophysics Geosystems G3
AN ELECTRONIC JOURNAL OF THE EARTH SCIENCES
Published by AGU and the Geochemical Society

Article
Volume 8, Number 4
25 April 2007
Q04N11, doi:10.1029/2006GC001474
ISSN: 1525-2027

Deep-dwelling foraminifera as thermocline temperature recorders

Caroline Cléroux, Elsa Cortijo, and Jean-Claude Duplessy
Laboratoire des Sciences du Climat et de l'Environnement, IPSL, Laboratoire Mixte, CEA-CNRS-UVSQ, Parc du CNRS, F-91198 Gif sur Yvette Cedex, France (caroline.cleroux@lsce.cnrs-gif.fr)

Rainer Zahn
Institució Catalana de Recerca i Estudis Avançats, ICREA i Universitat Autònoma de Barcelona, Institut de Ciencia i Tecnologia Ambientals, Edifici Cn, Campus UAB, E-08193 Bellaterra (Cerdanyola), Spain

[1] We measured the oxygen isotopic composition of the deep-dwelling foraminiferal species *G. inflata*, *G. truncatulinoides* dextral and sinistral, and *P. obliquiloculata* in 29 modern core tops raised from the North Atlantic Ocean. We compared calculated isotopic temperatures with atlas temperatures and defined ecological models for each species. *G. inflata* and *G. truncatulinoides* live preferentially at the base of the seasonal thermocline. Under temperature stress, i.e., when the base of the seasonal thermocline is warmer than 16°C, *G. inflata* and *G. truncatulinoides* live deeper in the main thermocline. *P. obliquiloculata* inhabits the seasonal thermocline in warm regions. We tested our model using 10 cores along the Mauritanian upwelling and show that the comparison of $\delta^{18}O$ variations registered by the surficial species *G. ruber* and *G. bulloides* and the deep-dwelling species *G. inflata* evidences significant glacial-interglacial shifts of the Mauritanian upwelling cells.

Components: 10,829 words, 12 figures, 3 tables.

Keywords: deep-dwelling foraminifera; depth habitat; isotopic temperature; thermocline; North Atlantic; Mauritanian upwelling.

Index Terms: 4813 Oceanography: Biological and Chemical: Ecological prediction; 4870 Oceanography: Biological and Chemical: Stable isotopes (0454, 1041); 4944 Paleoceanography: Micropaleontology (0459, 3030).

Received 8 September 2006; **Revised** 23 January 2007; **Accepted** 31 January 2007; **Published** 25 April 2007.

Cléroux, C., E. Cortijo, J.-C. Duplessy, and R. Zahn (2007), Deep-dwelling foraminifera as thermocline temperature recorders, *Geochem. Geophys. Geosyst.*, *8*, Q04N11, doi:10.1029/2006GC001474.

Theme: Past Ocean Circulation
Guest Editors: C. Kissel, L. Labeyrie, J. Lynch-Stieglitz, and O. Marchal

1. Introduction

[2] Quaternary climatic variations resulted in large ocean circulation changes associated with the atmospheric and sea surface temperature variations. Deep and intermediate water temperature changes can be reconstructed by isotopic or trace element analyses in benthic foraminifera [*Martin et*

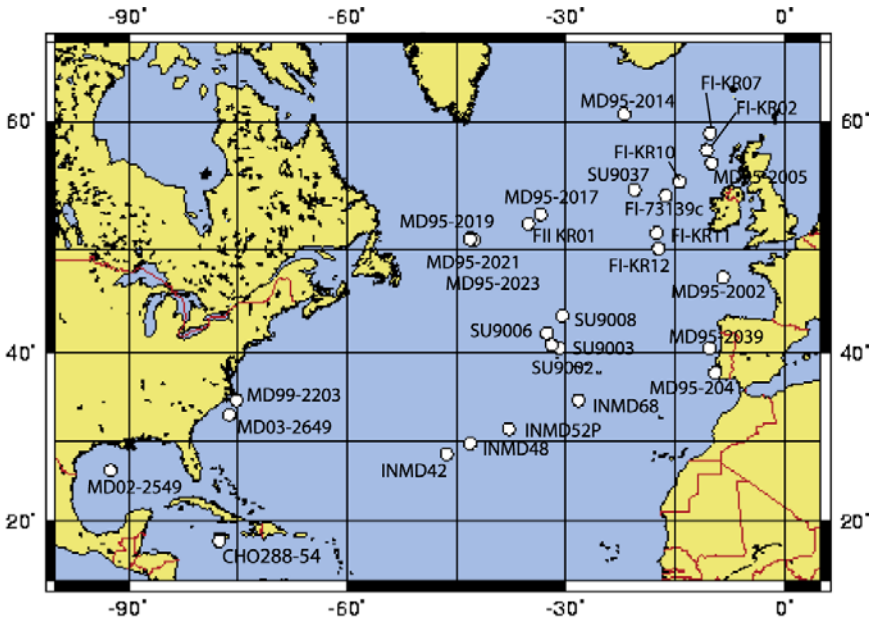

Figure 1. Locations and names of core tops. OMC, Martin Weinelt.

al., 2002; *Streeter and Shackleton*, 1979] or deep corals [*Schrag and Linsley*, 2002]. Assemblage analyses of fossil marine plankton communities, such as coccolithophores, surface dwelling foraminifera or diatoms are commonly used to infer past sea surface temperature [*Giraudeau et al.*, 2000; *Koç Karpuz and Schrader*, 1990; *Prell*, 1985]. However, little information is available on temperature variations in the upper 500 m of the water column, where most of the energy storage and heat transport occur [*Liu and Philander*, 2001].

[3] Deep-dwelling planktonic foraminifers inhabit the top few hundred meters of the ocean [*Bé*, 1977] and constitute potential recorders of thermocline conditions [*Fairbanks et al.*, 1980]. *Mulitza et al.* [1997] used the oxygen isotopic composition (δ^{18}O) of *G. truncatulinoides* to monitor past seawater temperature variations at 250 m depth and suggested that the thermal stratification of the western equatorial Atlantic was weaker during the Last Glacial Maximum (LGM) than during the Holocene.

[4] However, reconstructing mixed layer and thermocline structure requires insight into ecological niches of deep-dwelling planktonic foraminifers including their growth seasons and calcification depths. In this paper, we use multispecies δ^{18}O analyses to better constrain these parameters and to gain a fuller understanding of deep-dwelling foraminiferal habitats.

[5] We selected three species that are common in deep sea sediments: the transitional water species *Globorotalia inflata*, the warm and high salinity water species *Pulleniatina obliquiloculata* and the deep species *Globorotalia truncatulinoides* right and left coiling [*Bé*, 1977]. δ^{18}O values of these species sampled in modern core tops are used to calculate isotopic temperature (Tiso). These values constrain their calcification depths and seasonalities, when compared to modern hydrological data. We apply this concept to down-core isotope profiles from a suite of sediment cores from the Mauritanian margin to assess upwelling intensity during the LGM.

2. Samples and Methods

[6] We measured the oxygen isotopic composition of foraminifer shells from 29 core tops raised from the subtropical to northern North Atlantic, 28°–61°N (Figure 1). The samples cover three marine climatological regimes: the North Atlantic Current, the warm and well-stratified subtropical gyre and the deep mixed-layer zone in the north.

[7] Except for the 4 southernmost cores (centered around 30°N), the stratigraphy of all the cores

Table 1. Location, Water Depth, Age Control, and SST From Database and Surface-Dwelling Species[a]

Core Top	Latitude, °N	Longitude, °W	Depth, m	Age Control MARGO[b]	References[c]	Summer SST[d]	Foraminifera SST[e]
CHO 288 54	17°25	77°39	1020	1	1	28.6	29.6
MD 02-2549	26°25	92°33	2049	4	3	29.2	28.7
INMD 42BX-8[f]	28°34	46°21	3774	3 and 4	1, 2	26.9	22.9
INMD 48BX-1[f]	29°48	43°13	2836	3 and 4	1, 2	26.4	23.3
INMD 52 P[f]	31°31	37°52	3631			26	25
MD03-2649	33°11	76°15	958	4	3	27.9	29.7
INMD 68BX-6[f]	34°48	28°21	2520	3 and 4	1, 2	24	21.4
MD99-2203	34°58	75°12	620	1	3	27.1	27.3
MD95 2041	37°50	09°30	1123	3 and 4	2, 3	19.2	17.9
MD95 2039	40°34	10°20	3381	3	2	19.2	17.9
SU 9002 P	40°34	30°56	2220	3	2	22	16.8
SU 9003 P	40°5	32	2478	2 and 3	2, 3	22.1	20.2
SU 9006 P	42°	32	3510	3	2	21.7	19
SU 9008 P	43°5	30°35	3080	3 and 4	2, 3	20.1	20.3
MD95 2002	47°27	08°32	2174	3 and 4	2, 3	17.9	16.8
F I KR 12	50°15	17°37	4787	3 and 4	1, 2	13.4	14.2
MD95 2021	50°51	42°44	4283	3	2	13.6	12.3
MD95 2023	50°58	43°13	4198	3	2	13.6	13
MD95 2019	51°05	43°13	4262	3	2	11.6	12
F I KR 11	51°48	17°68	4654	3 and 4	1, 2	15.4	14.4
F II KR 01	52°28	35°25	3886	3 and 4	1, 2	12	10.1
MD95 2017	53°02	33°31	3100	3	2	12.5	9.7
F I 139 c	54°38	16°21	2209	1	1	14.3	14.6
SU 9037 S	55°06	20°44	2676	3	2	14	13.2
F I KR 10	55°6	14°48	2216	3 and 4	1, 2	13.9	13.6
MD95 2005	57°02	10°03	2130	3 and 4	2, 3	13.6	12.3
F I KR 02	58°08	10°72	2005	3	2	13.2	12.5
F I KR 07	59°25	10°22	482	3	2	12.7	11.5
MD95 2014	60°34	22°04	2397	3 and 4	2, 3	11.6	10.6

[a] Quality of age control according to the four levels defined in MARGO and references. The two last columns allow comparison between modern sea surface temperature (SST) and isotopic temperature of surface-dwelling species.
[b] Chronostratigraphic quality levels go from 1 to 4 with different levels of uncertainty: Numbers 1 and 2 are for radiometric control within the intervals 0–2 ka and 0–4 ka, respectively, level 3 is used for specific stratigraphic control (like % *Globorotalia hirsuta* left coiling), and number 4 represents other stratigraphic constraints [*Kucera et al.*, 2005].
[c] References: 1, Core top included in MARGO database; 2, J. Duprat, personal communication, 2006; 3, LSCE database.
[d] From World Ocean Atlas.
[e] Mean isotopic temperature measured on *G. ruber* or *G. bulloides*. Mean one sigma range is about 1°C.
[f] Cores with no downcore stratigraphy.

indicates that the upper part correspond to an expanded Holocene section. This minimizes the influence of upward bioturbational mixing of older foraminiferal shells (from early Holocene or deglaciation). However, for all the cores, we use the Late Holocene stratigraphic quality levels as defined in MARGO [*Kucera et al.*, 2005] to ensure an Upper Holocene age of the samples and checked that the isotopic composition of the surface-dwelling species *G. ruber* and *G. bulloides* are consistent with modern seawater temperature and salinity (Table 1).

[8] Foraminifera were picked in different sizes fractions. *G. ruber* and *G. bulloides* were chosen in the 250–315 μm fraction. About 4 shells were taken for each δ^{18}O analysis. Deep-dwelling species were picked in the 355–400 μm fraction. *G. inflata* specimens were also taken in the 250–315 μm size fraction to check for a possible size effect. 2 or 3 tests were used for analyses. 2 to 10 isotopic measurements on the same sample were performed to estimate the δ^{18}O variability within single sediment samples (Table S1[1]).

[9] Prior to analysis, shells were ultrasonically cleaned in methanol to remove clays and other impurities and then roasted at 380°C during 30 min under vacuum to burn organic matter. Samples

[1] Auxiliary materials are available at ftp://ftp.agu.org/apend/gc/2006gc001474.

were analyzed using Finnigan MAT 251 mass spectrometer equipped with an automated Kiel CARBO device for CO_2 production. We used both NBS 19 and NBS 18 as reference standards to ensure calibration over a large range of $\delta^{18}O$ values [*Ostermann and Curry*, 2000]. All results are expressed as $\delta^{18}O$ in ‰ versus V-PDB. The mean external reproducibility of carbonate standards is 0.07‰ for $\delta^{18}O$, this error is insignificant in our calculation.

3. Calcification Temperature Estimates

[10] Several authors have shown that many foraminiferal species do not precipitate their shell in isotopic equilibrium with ambient water but exhibit an offset called "vital effect" that is assumed to be constant. For surface-dwellers vital effect seems to be constant both within the same species across its optimum environmental regimes [*Duplessy et al.*, 1991; *Wang et al.*, 1995] and through stratigraphic time. For deep-dwelling species, contradictory results have been published in the literature. However, apparent disequilibria are rather small in the range 0 ± 0.3‰ [*Deuser and Ross*, 1989; *Fairbanks et al.*, 1980; *Ganssen*, 1983; *Niebler et al.*, 1999; *Wilke et al.*, 2006] which is equivalent to ±1°C.

[11] Neglecting isotopic equilibrium, we first quantify the depth habitat of the deep-dwelling species and then test the robustness of this approach by calculating the effect of a potential disequilibrium for each species.

[12] We calculated Tiso using the paleotemperature equation of *Shackleton* [1974] (equation (1)). This relation fits isotope measurements performed on benthic foraminifera and the slope of this relationship fits well with measurements performed on planktonic species [*Bemis et al.*, 1998; *Bouvier-Soumagnac and Duplessy*, 1985].

$$T_{isotopic} = 16.9 - 4.38 * \left(\delta^{18}O_{foraminifera} - \delta^{18}O_{seawater}\right) + 0.1 * \left(\delta^{18}O_{foraminifera} - \delta^{18}O_{seawater}\right)^2 \quad (1)$$

This equation does not differ from other paleotemperature equations [*Epstein et al.*, 1953; *Kim and O'Neil*, 1997] by more than 0.8°C in the range 8–20°C.

[13] In this equation, $\delta^{18}O$ of both foraminifera and water are measured against the same working standards. As we report here foraminifera $\delta^{18}O$ against V-PDB and seawater $\delta^{18}O$ against V-SMOW, a 0.27‰ correction factor was used to account for the difference between PDB-CO_2 and SMOW-CO_2 standards [*Hull and Turnbull*, 1973; *Hut*, 1987].

[14] We extracted salinity data from the World Ocean Atlas 2001 (WOA) [*Conkright et al.*, 2002] to estimate the $\delta^{18}O_{seawater}$ value for each core top sample. We use the Goddard Institute for Space Studies database for the North Atlantic (http://data.giss.nasa.gov/o18data) to compute the relationship between $\delta^{18}O_{seawater}$ and salinity in the North Atlantic Ocean between 0 and 500 meter depth. This gives a relationship very close to the GEOSECS equation defined between 0 and 250 m:

$$\delta^{18}O_{seawater} = -19.264 + 0.558 * \text{salinity} \quad (\text{in V-SMOW}) \quad (2)$$

At high latitude, salinity is nearly constant in the mixed layer and the thermocline. We calculated $\delta^{18}O_{seawater}$ from the mean salinity value between 0 and 500 m (Figure A1). The same approach is applied for low latitude cores. In the subtropical gyre, salinity varies from 37 psu at the surface to 35.75 psu at 500 m depth. Taking a mean salinity/$\delta^{18}O$ value for the water column results in an error on the isotopic temperature of ±1.5°C, which is small when compared to the observed temperature range within the thermocline which commonly exceed 10°C. Taking into account the experimental error of ±0.07‰ on the isotope measurement, the total error is about ±2°C.

[15] This calculation rests on the assumption of isotopic equilibrium of foraminifer carbonate shells with ambient seawater. If we assume a vital effect of ±0.3‰, which is the maximum value given by previous studies [*Niebler et al.*, 1999], isotopic temperatures will change by less than 1.5°C according to the paleotemperature equation (1). Given the large scatter of the measured $\delta^{18}O$ values, such a small disequilibrium would not affect our conclusions.

4. Results and Discussion: A Modern Ecological Concept

[16] To compare Tiso with modern temperatures from atlas we applied the following method: To take account regional variability, we extracted, around each core, summer and winter temperature profiles from the four neighboring grid points. Figure 2 gives an example for the isotopic results of *G. inflata* in the core FI KR02 but we applied

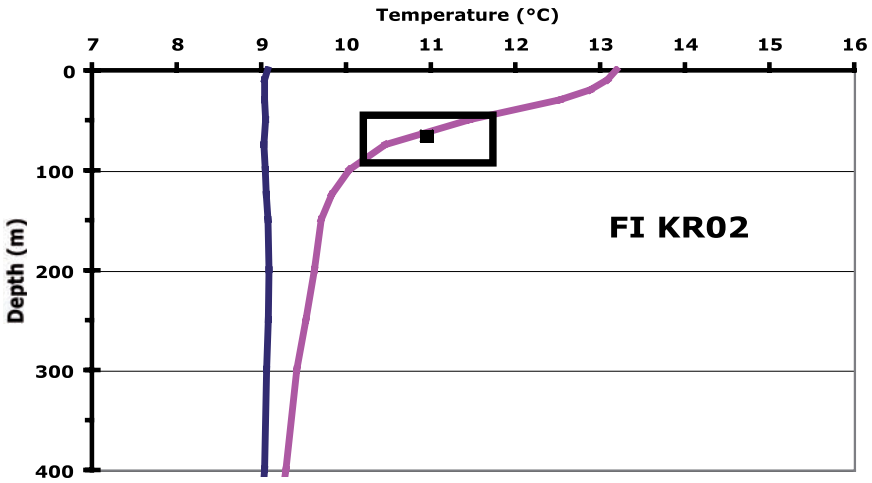

Figure 2. Comparison of the mean isotopic temperature (Tiso) of *G. inflata* with modern temperatures for the core FI KR02. Blue (pink) line is the coldest winter (warmest summer) temperature profile from WOA 2001. Square represents the mean Tiso. Rectangle indicates the possible habitat depth. The width of rectangle gives the one sigma range in Tiso resulting from replicate $\delta^{18}O_{foraminifera}$ measurements. The height of rectangle expresses this error in terms of water depth.

the same method for each core top and each species (Figures A2, A3, and A4).

[17] At midlatitudes and high latitudes, the Tiso of all species are higher than winter temperatures but coincide with summer temperatures around the base of the summer thermocline (BST hereinafter, which we define as the depth where the summer and winter profiles join). In agreement with the observation that planktonic blooms occur during summer time [*Colebrook*, 1982; *Esaias et al.*, 1986]. At low latitude, we cannot exclude the possibility of a surface habitat during winter based on our isotopic measurements [*Deuser*, 1987; *Deuser and Ross*, 1989; *Deuser et al.*, 1981].

4.1. *G. inflata*

[18] As results were similar for both size fractions (250–315 μm and 355–400 μm) we have combined the two data sets (Table S1). We defined the different ecological niches according to local hydrology. We have separated the water column into three units: the seasonal thermocline, the BST, and the main thermocline below this level.

[19] When the BST is colder than about 16°C, Tiso of *G. inflata* corresponds to the temperature at the BST (Figures A2a to A2u). When the BST is warmer than 16°C, Tiso of *G. inflata* indicates a deeper habitat, in the upper part of the main thermocline (Figures A2v to A2y). In the latter case, it is impossible to determine whether this species lives throughout the year or only seasonally, because the temperature at this depth exhibits little seasonal variation.

[20] We develop a simple concept for this species: when the Tiso of *G. inflata* is lower than 16 ± 1°C, we consider that it records the temperature at the BST. When the Tiso is higher than 16 ± 1°C, it reflects warm conditions in the upper part of the main thermocline.

[21] Our ecological model is in agreement with several in-situ observations. In plankton tows and surface sediment studies from off NW Africa, *Ganssen* [1983] and *Ganssen and Sarnthein* [1983], used isotope differences between *G. ruber* and *G. inflata* to mirror seasonal temperature changes. As *G. ruber* lives during the warm season and *G. inflata* at the BST, of which temperature is close to that of winter condition, this interpretation fits well with our concept. The development of this species during warm season at midlatitude is confirmed by the plankton nets of *Ottens* [1992] collected between 30°N and 60°N in the Atlantic. Recently, living *G. inflata* were sampled in the SW-African margin water column during austral summer [*Wilke et al.*, 2006]. In this study they found a maximum for both the shell concentrations and the amount of calcification within the thermocline. From 1978 to 1984, Deuser and colleagues studied sediment traps in the Sargasso Sea and

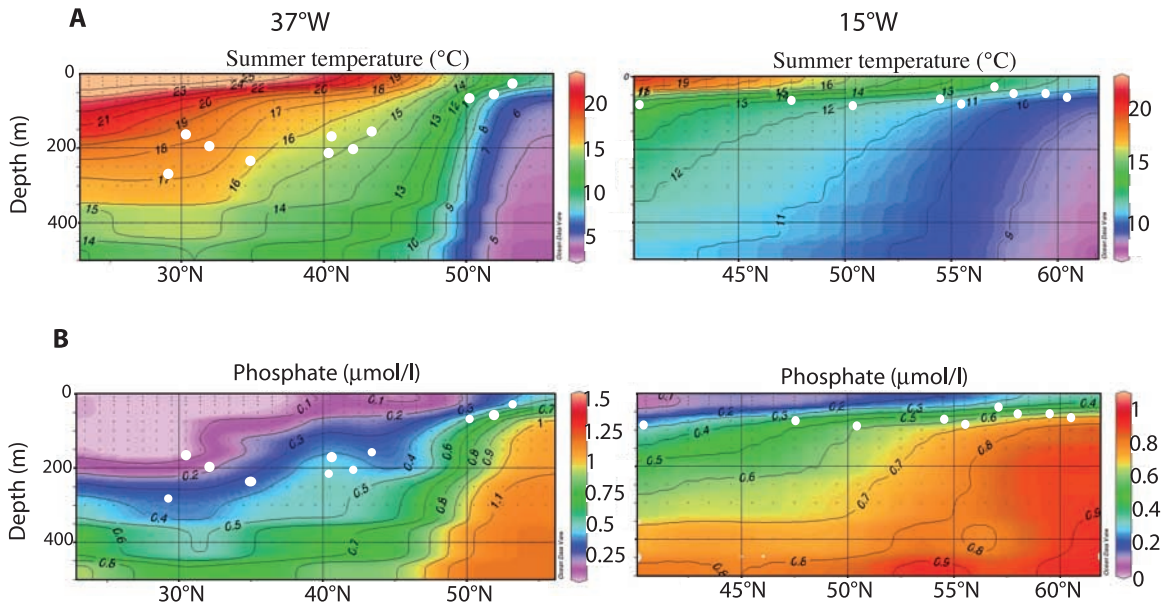

Figure 3. Depth positions of *G. inflata* 355–400 μm on summer temperature (°C) and phosphate (μmol/l) cross section at (left) 37°W and (right) 15°W. *G. inflata* depth habitats (white circle) were placed according to latitude of their core top and calculated Tiso on (a) two longitudinal temperature sections and (b) corresponding PO_4 section.

made oxygen isotopic measurements and foraminifer fluxes observations [*Deuser*, 1987; *Deuser and Ross*, 1989; *Deuser et al.*, 1981]. They concluded that *G. inflata* lives in the winter mixed-layer. This result is in agreement with our observations at low latitude and provides additional information on the life season in this warm region. Plankton tows studies in the equatorial Atlantic show maximum abundance of *G. inflata* at the BST [*Ravelo and Fairbanks*, 1990] and oxygen isotopic measurements confirm this calcification depth [*Ravelo and Fairbanks*, 1992]. Finally the ecological niche defined in our study for *G. inflata* agrees with the calcification depth observed in the North Atlantic [*Durazzi*, 1981; *Ganssen and Kroon*, 2000; *Mortyn and Charles*, 2003].

[22] Along longitudinal sections across the North Atlantic, we found that the depth habitat of *G. inflata* follows the 0.3–0.4 μMol/l PO_4 concentration line in seawater (Figure 3). The BST is indeed a level of nutrient accumulation [*Sarmiento et al.*, 2004] and concentration of phytoplankton is high, providing food for foraminifera.

4.2. *G. truncatulinoides* Dextral and Sinistral

[23] Both *G. truncatulinoides* right and left coiling exhibit roughly similar Tiso (Table S1) and therefore occupy the same ecological niche. *Ganssen and Kroon* [2000] have also found similar $\delta^{18}O$ for both coiling directions. However, we still separate them because they constitute different genetic species [*de Vargas et al.*, 2001] and they have different behavior with respect to trace element incorporation (C. Cléroux et al., manuscript in preparation, 2007). In our data set, *G. truncatulinoides* right coiling has a greater temperature tolerance than *G. truncatulinoides* left coiling: the standard deviation of the Tiso at a given location is often larger for the right coiling form than for the left coiling (Figures A3i to A3m and A3r).

[24] When the BST is colder than about 16°C, *G. truncatulinoides* is found in the seasonal thermocline lower part (Figures A3a to A3n). When the BST is warmer than about 16°C, *G. truncatulinoides* lives deeper in the main thermocline (Figures A3o to A3t). Although *G. truncatulinoides* and *G. inflata* have similar depth habitat, *G. truncatulinoides* always lives at greater depth than *G. inflata* when both species are present in the same area. The great scatter of the calculated Tiso for low latitude samples reflects the wide temperature variation that occurs in the upper water column.

[25] We thus develop a concept similar to that of *G. inflata*: when the Tiso of *G. truncatulinoides* is

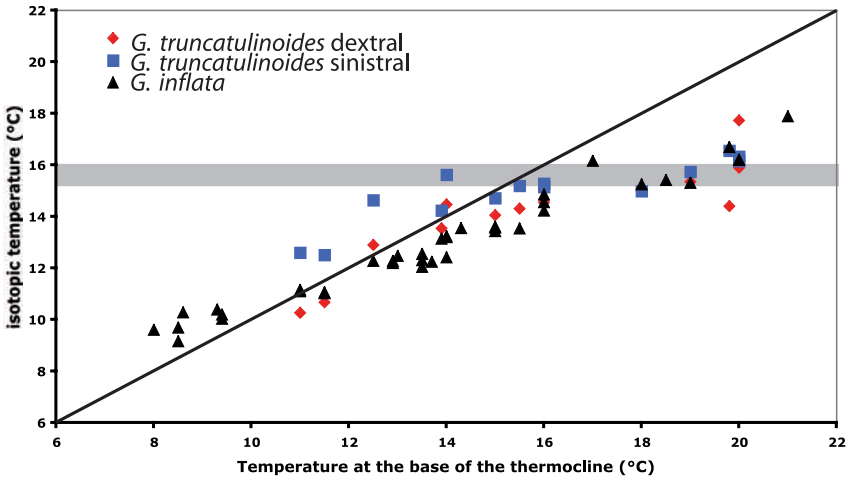

Figure 4. Tiso of *G. inflata* (black triangle), *G. truncatulinoides* dextral (red diamond), and sinistral (blue square) from *Ganssen and Kroon* [2000] versus temperature at the base of the summer thermocline extracted from modern atlas at their box core locations. Line of slope 1 is plotted. The gray area, from 15.7°C to 16°C, underlines the temperature threshold from which Tiso are no more equal to temperature at the BST.

lower than 16 ± 1°C, we consider that it records the temperature at the BST. When the Tiso is higher than 16 ± 1°C, it reflects conditions of the main thermocline.

[26] Local hydrology therefore fixes the depth habitat of *G. truncatulinoides*. *LeGrande et al.* [2004] predict *G. truncatulinoides* $\delta^{18}O$ for many South and North Atlantic core tops assuming (1) a single depth calcification at 350 m or (2) 30% of calcification at the surface and 70% of calcification at 800 m. We tested our concept with the North Atlantic data of *LeGrande et al.*'s [2004] paper. One fraction of their data comes from the study of *Ganssen and Kroon* [2000] and will be discussed further in the text. The other fraction corresponds to core tops located in warm regions, around the equator or in the Gulf stream water, where temperature at the BST largely exceed our threshold value of 16°C. Thus, according to our prediction, *G. truncatulinoides* calcifies in the main thermocline, in agreement with the model of *LeGrande et al.* [2004], which specifies that it is around 350 m. On the contrary, our concept does not fit with the South Atlantic *LeGrande et al.* [2004] data. Estimated isotopic temperatures are very low, in contradiction with the temperature preferences known for the North Atlantic *G. truncatulinoides*. It is possible that the genetic difference observed by *de Vargas et al.* [2001] between the North and South Atlantic *G. truncatulinoides* corresponds to different ecological characteristics. We do not have elements to check that hypothesis and we consider that at the present stage the concept is not adapted for the South Atlantic.

[27] Our concept directly reproduces regional observations. In the Sargasso Sea, $\delta^{18}O$ values of *G. truncatulinoides* record average conditions near 200 meters depth [*Deuser*, 1987; *Deuser and Ross*, 1989; *Deuser et al.*, 1981; *McKenna and Prell*, 2004]. This depth corresponds to the BST with a temperature close to 16°C. Here, *G. truncatulinoides* inhabits its preferred habitat. In slope water, cold core rings of the Gulf Stream and Northern Sargasso Sea plankton tows, *Fairbanks et al.* [1980] observed that the main population of *G. truncatulinoides* is found between 125 to 175 m, which corresponds to the BST. *Mulitza et al.* [1999] also showed that *G. truncatulinoides* lives in phosphate-rich waters and is a good recorder of thermocline nutrient levels.

[28] To compare more easily our concept with previous studies, we apply our strategy and recalculate Tiso for *G. truncatulinoides* and *G. inflata* from the data of *Ganssen and Kroon* [2000]. Tiso for *G. truncatulinoides* and *G. inflata* follows the temperature at the BST up to 15.7°C ± 0.3 (Figure 4). Above this temperature, Tiso become too low and reflect the sinking of the foraminifera in the main thermocline.

Table 2. Summary of Ecological Model for the Three Deep-Dwelling Foraminifera Species: *G. inflata*, *G. truncatulinoides*, and *P. obliquiloculata*

Species	Preferred Habitat	Temperature Threshold	Stress Habitat
G. inflata	base of the seasonal thermocline	16°C	Upper part of the main thermocline
G. truncatulinoides dextral and sinistral	base of the seasonal thermocline	16°C	Main thermocline
P. obliquiloculata	base of the seasonal thermocline	–	–

4.3. *P. obliquiloculata*

[29] *P. obliquiloculata* has a restricted geographical distribution and was found in only 7 core tops. Tiso of *P. obliquiloculata* reflect those at the BST (Figures A4a to A4g). This species inhabits the same ecological niche as *G. inflata* but is restricted to warm regions. In a core located south of Cuba (core CHO288-54, Figure A4f), *P. obliquiloculata* is in equilibrium with the seawater temperature at 175 m depth. In this region where seasonality is quasi-absent and stratification is strong throughout the year, this depth corresponds to the base of the upper thermocline.

[30] *Ravelo and Fairbanks* [1992] found the maximum occurrence of *P. obliquiloculata* at 60 m in equatorial Atlantic waters, i.e., at the BST. In a study off NW Africa, *Ganssen* [1983] concludes also that *P. obliquiloculata* delineates winter temperature. Except for one specimen collected in March, this species was not found in winter plankton tows. Moreover, calculated Tiso from sediment samples was often a little warmer than winter sea surface temperature thus compatible with temperature at the BST. In the Sargasso Sea, the sediment traps studies of [*Deuser*, 1987; *Deuser and Ross*, 1989; *Deuser et al.*, 1981] yield a characteristic isotopic depth of 0–75 m which do not contradict these results.

[31] As the preferred habitat for all species discussed here is at the BST (Table 2), we compared Tiso with modern temperatures at the BST (ΔT), at each core-top location (Figure 5). In a foreseeable way, for the maximum number of analysis, Tiso of *G. inflata* and *P. obliquiloculata* is equal to the temperature at the BST ($\Delta T = 0$). In the histogram of *G. truncatulinoides* the higher peak is for $\Delta T = -1$ reflecting our observation that this species calcifies always a little deeper than *G. inflata*. *P. obliquiloculata* has a symmetric histogram because it has only one depth habitat. On the contrary, *G. truncatulinoides* and *G. inflata* have distorted histograms toward negative values representing their stress habitats in the main thermocline.

5. Reconstruction of the Glacial Thermocline Structure Off Northwest Africa

[32] We selected 10 cores collected along the Northwest African margin from 15°N to 35°N within the Mauritanian upwelling regime (Figure 6) [*Zahn*, 1986]. Data are reported in Table 3. Two cores (M12-328 and M16-030) are located in the today's center of perennial upwelling (Figure 6), cores M13-289 and M12-347 south of this zone and M15-637 outside. Others cores are distributed along the coast, north of the maximum intensity upwelling area. $\delta^{18}O$ of *G. ruber*, *G. bulloides* and *G. inflata* has been analyzed previously [*Zahn*, 1986] for the Holocene and LGM using benthic $\delta^{18}O$ for stratigraphy [*Sarnthein et al.*, 1994; *Zahn and Sarnthein*, 1987]. *G. bulloides* is a surface-dwelling species typical of upwelling season. This species provides seawater temperature estimates for that period [*Ganssen*, 1983; *Ganssen and Kroon*, 2000; *Ganssen and Sarnthein*, 1983; *Zahn*, 1986]. *G. ruber* lives in the surface mixed layer during the warm season [*Ganssen and Kroon*, 2000]. We derive Tiso from these $\delta^{18}O$, using modern seawater $\delta^{18}O$ values for Holocene data and already reconstructed LGM seawater $\delta^{18}O$ for the same cores, or for very nearby cores, for LGM data [*Duplessy et al.*, 1991]. Results are reported in Table 3. We used the same method developed for the construction of our concepts to compare Holocene Tiso and modern temperatures from atlas (Figure A5). For all cores, the calculated Holocene Tiso of *G. inflata* are close to the threshold value of 16°C and nicely fit with those of the BST along the

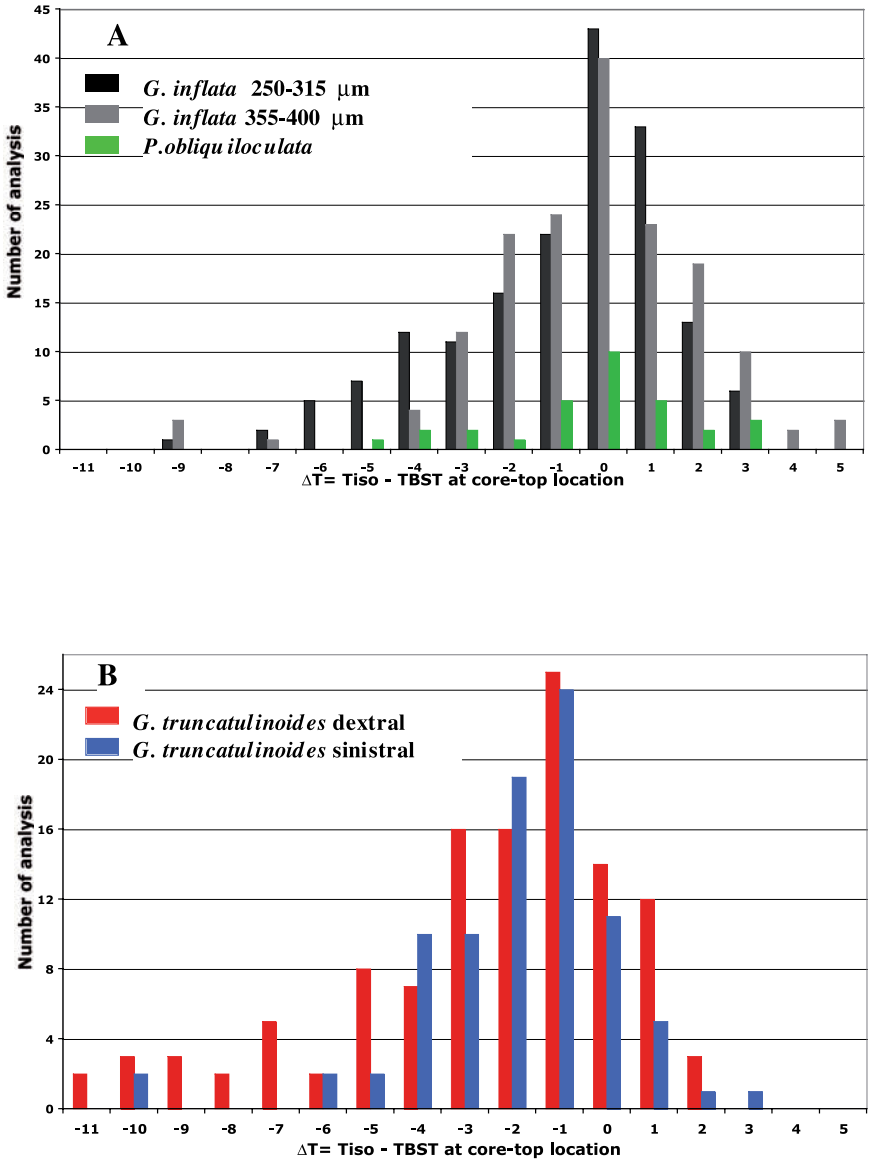

Figure 5. Histogram of the difference between Tiso and the modern temperature at the base of seasonal thermocline (TBST) from WOA 2001 at each core-top location for (a) *G. inflata* and *P. obliquiloculata* and (b) the two coiling directions of *G. truncatulinoides*.

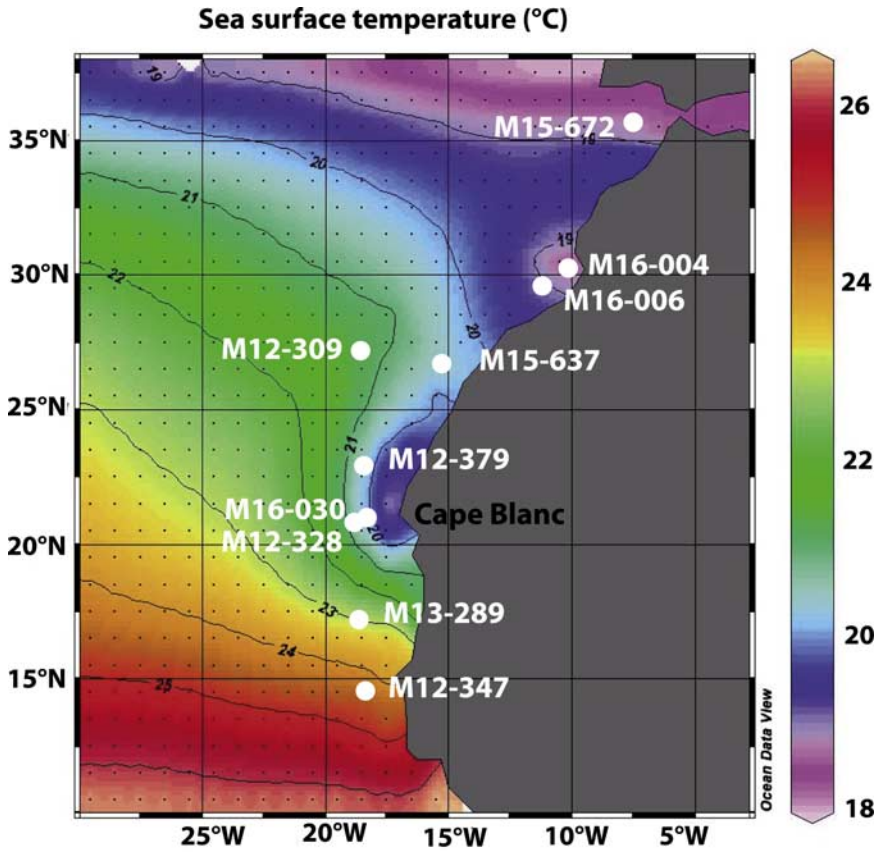

Figure 6. Sea surface temperatures and locations of the cores used to reconstruct upwelling intensity along the NW African margin.

Northwest African Margin (Figure A5). We highlighted in this paper that *G. inflata* might change his depth habitat when seawater becomes warmer; as Tiso for LGM samples are colder than the present we assume that *G. inflata* did not change its habitat from LGM time to Holocene. Accordingly, we consider that the calculated LGM Tiso reflect conditions at the BST.

[33] The upwelling activity, which exist at the cores M12-328, M16-030 and M16-004 locations (Figures 6 and 7), is reflected by several indicators: Tiso of *G. bulloides* are low; Tiso of *G. inflata* are also low because the temperature at the BST is linked to the coldest month conditions. Thus Tiso differences between *G. bulloides* and *G. inflata* under upwelling conditions are small. We shall use the whole set of these indicators to characterize upwelling activity. In the other cores, outside the main upwelling cell, mean Tiso of *G. bulloides* is about 21°C (M13-289, M12-309 and M16-006). The absence of upwelled cold water is well marked between 23°N and 29°N with the warm Tiso of *G. inflata* (Figure 7).

[34] During LGM, in the southern cores M12-347 and M13-289, Tiso of *G. inflata* are low (about 12.5°C), whereas those of *G. bulloides* are high (19.1°C and 19.5°C, respectively), resulting in large temperature difference between *G. bulloides* and *G. inflata* (6.9°C and 6.6°C). This suggests that the strong cooling observed at the BST is not associated with upwelling during glacial conditions but is probably due to a water mass circulation different from the present [*Sarnthein et al.*, 1994].

[35] In the cores M12-328, M16-030, M12-379 and M12-309, Tiso for *G. inflata* is comprised between 14°C and 15°C, and the mean Tiso of *G. bulloides* is 19°C. The mean temperature difference between the two species is about 4.5°C. According to Holocene observations, it reflects hydrological area with moderate upwelling activity. We conclude that during LGM, upwelling activity

Table 3. Characteristics of the NW African Margin Cores, Oxygen Isotopic Data, Oxygen Isotopic Composition of the Water, and Calculated Isotopic Temperature for Holocene and LGM Periods[a]

				Holocene								LGM						
Core	Latitude, °N	Longitude, °W	Depth, m	$\delta^{18}O$ *G. ruber*[b]	$\delta^{18}O$ *G. inflata*[b]	$\delta^{18}O$ *G. bulloides*[b]	$\delta^{18}O$ sea SMOW[c]	T* *G. ruber*	T* *G. inflata*	T* *G. bulloides*	ΔT *G. bulloides*-*G. inflata*	$\delta^{18}O$ *G. ruber*[b]	$\delta^{18}O$ *G. inflata*[b]	$\delta^{18}O$ *G. bulloides*[b]	$\delta^{18}O$ seawater SMOW[d]	T* *G. ruber*	T* *G. inflata*	T* *G. bulloides*	ΔT *G. bulloides*-*G. inflata*
M15-672	34.51	8.07	2455	−0.22	0.85		1.08	21.5	16.7			1.85	2.70	2.31	2.15	17.0	13.4	15.0	1.7
M16-004	29.58	10.38	1512	−0.24	0.90	0.29	1.02	21.3	16.2	18.9	2.7	1.81	2.58	1.83	2.18	17.3	14.0	17.3	3.2
M16-006	29.14	11.29	796	−0.04	0.67	−0.15	1.10	20.8	17.6	21.3	3.7	1.84	2.50	1.56	2.18	17.2	14.4	18.4	4.1
M15-637	27	18.59	3849	−0.71	0.65		1.29	24.8	18.5			1.51	2.46	1.88	2.41	19.7	15.5	18.0	2.5
M12-309	26.5	15.06	2820	−0.36	0.50	−0.03	1.12	22.3	18.4	20.8	2.4	1.45	2.38	1.32	2.21	19.1	15.0	19.7	4.7
M12-379	23.08	17.44	2136	−0.64	0.61		1.12	23.6	18.0			1.25	2.59	1.55	2.18	19.8	14.0	18.5	4.5
M16-030	21.14	18.03	1500	−1.13	0.84	1.05	0.92	25.0	16.1	15.2	−0.9	0.49	2.44	1.44	2.18	23.3	14.6	19.0	4.4
M12-328	21.08	18.34	2778	−1.00	0.74	0.26	0.91	24.4	16.5	18.6	2.1	0.84	2.53	1.53	2.18	21.7	14.2	18.6	4.4
M13-289	18.04	18.01	2490	−1.19	0.90	−0.20	0.85	25.0	15.5	20.4	4.9	0.99	2.92	1.40	2.16	20.9	12.5	19.1	6.6
M12-347	15.5	17.52	2576	−1.38	0.72		0.77	25.5	15.9			1.16	2.81	1.23	2.08	19.8	12.6	19.5	6.9

[a] For both periods, isotopic temperature difference between *G. bulloides* and *G. inflata* is calculated. T*, isotopic temperature.
[b] From *Zahn* [1986].
[c] From World Ocean Atlas.
[d] From *Duplessy et al.* [1991].

disappeared or was strongly reduced between 21°N and 26.5°N. In agreement with these data, a productivity smaller than today was deduced for the LGM in an extensive study of the coastal upwelling off Cape Blanc [*Bertrand et al.*, 1996; *Martinez et al.*, 1999].

[36] For the northern cores (M15-637, M16-006, M16-004 and M15-672) the reconstructed LGM Tiso for *G. bulloides* are the lowest (17.2°C in mean) and the Tiso differences between *G. bulloides* and *G. inflata* are small (2.9°C) compared to southern cores. We interpret these data as an evidence for enhanced upwelling activity, in agreement with stronger LGM productivity off Morocco [*Freudenthal et al.*, 2002]. The shift of the main upwelling cell to the north, which is also seen in changes of coccolith morphology and distribution [*Henderiks and Bollman*, 2004] reflects the enhanced trade winds intensity about 36°N to 24°N during LGM [*Hooghiemstra et al.*, 1987].

6. Conclusions

[37] We propose here a simple ecological concept to constrain the habitat and seasonality for *G. inflata*, *G. truncatulinoides* right and left coiling and *P. obliquiloculata*, based on the comparison between isotopic temperatures in North Atlantic core tops and modern atlas data. These species inhabit preferentially the base of the seasonal thermocline. Under high temperature stress, *G. inflata* and *G. truncatulinoides* sink within the main thermocline to reach colder waters. These depth habitats correspond to abundant phytoplankton level that provides food for these large non-symbiotic foraminifera. This ecological concept fits well with previous in-situ studies.

[38] The depth habitat of these species in the water column is now well-characterized. Paired analyses of surface and deep-dwelling planktonic foraminifera along a single sediment core offers possibility to reconstruct temperature at critical levels of the water column, i.e., the surface and base of the thermocline. We have tested this concept under glacial conditions using several cores raised off West Africa. By comparison with the modern pattern, our results show a shift of the main upwelling cells from Cape Blanc to Morocco and Canary basin during the LGM. Agreement between this conclusion and previous micropaleontological reconstructions indicates that our ecological concept should be valid back in time.

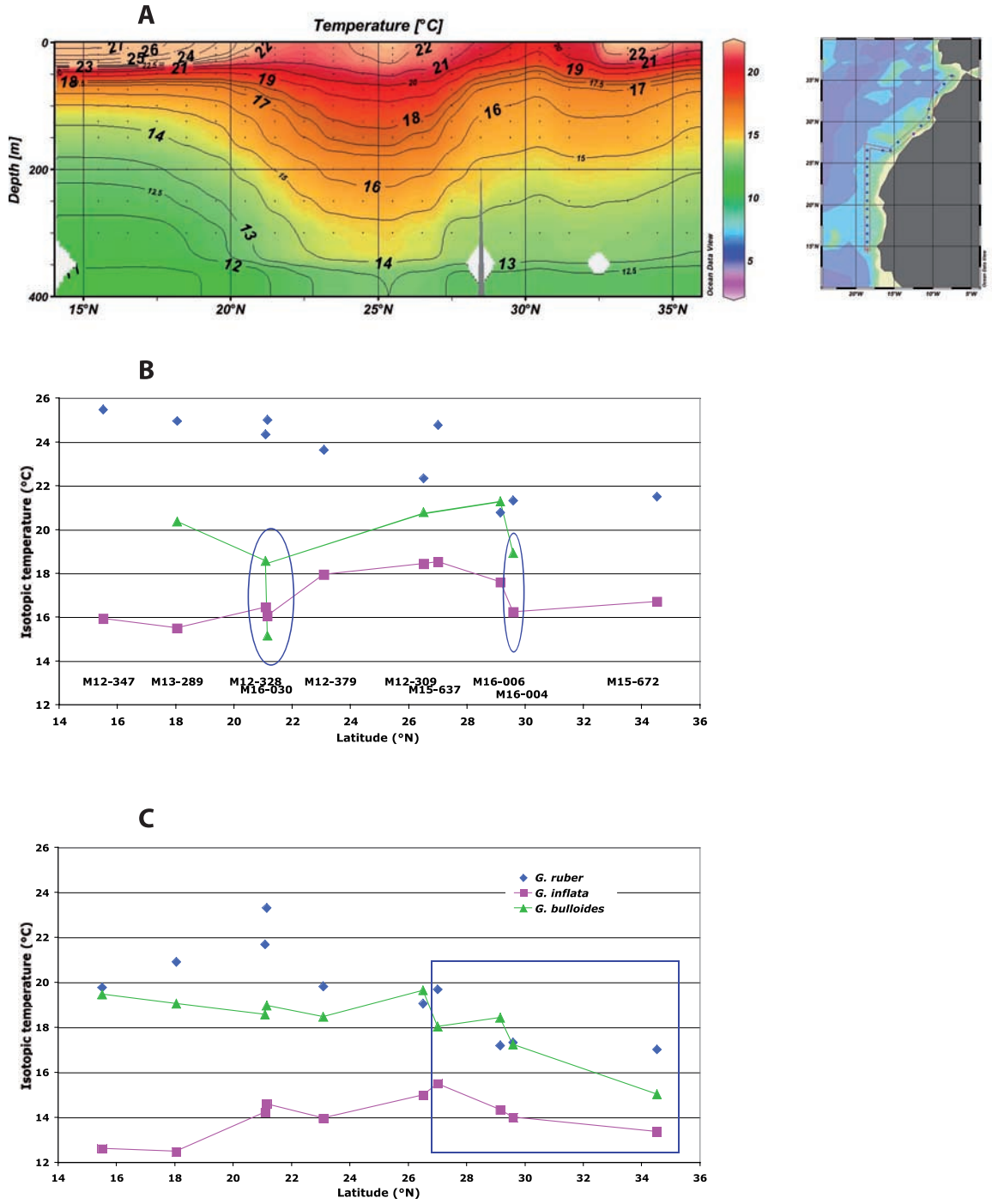

Figure 7. (a) Summer temperature versus depth for a section which passes through each core location (see map). (b) Holocene Tiso of *G. ruber* (blue), *G. bulloides* (green), and *G. inflata* (pink) in a latitudinal transect. (c) LGM Tiso for the same species. Blue circles and rectangle underline location of the main upwelling cells.

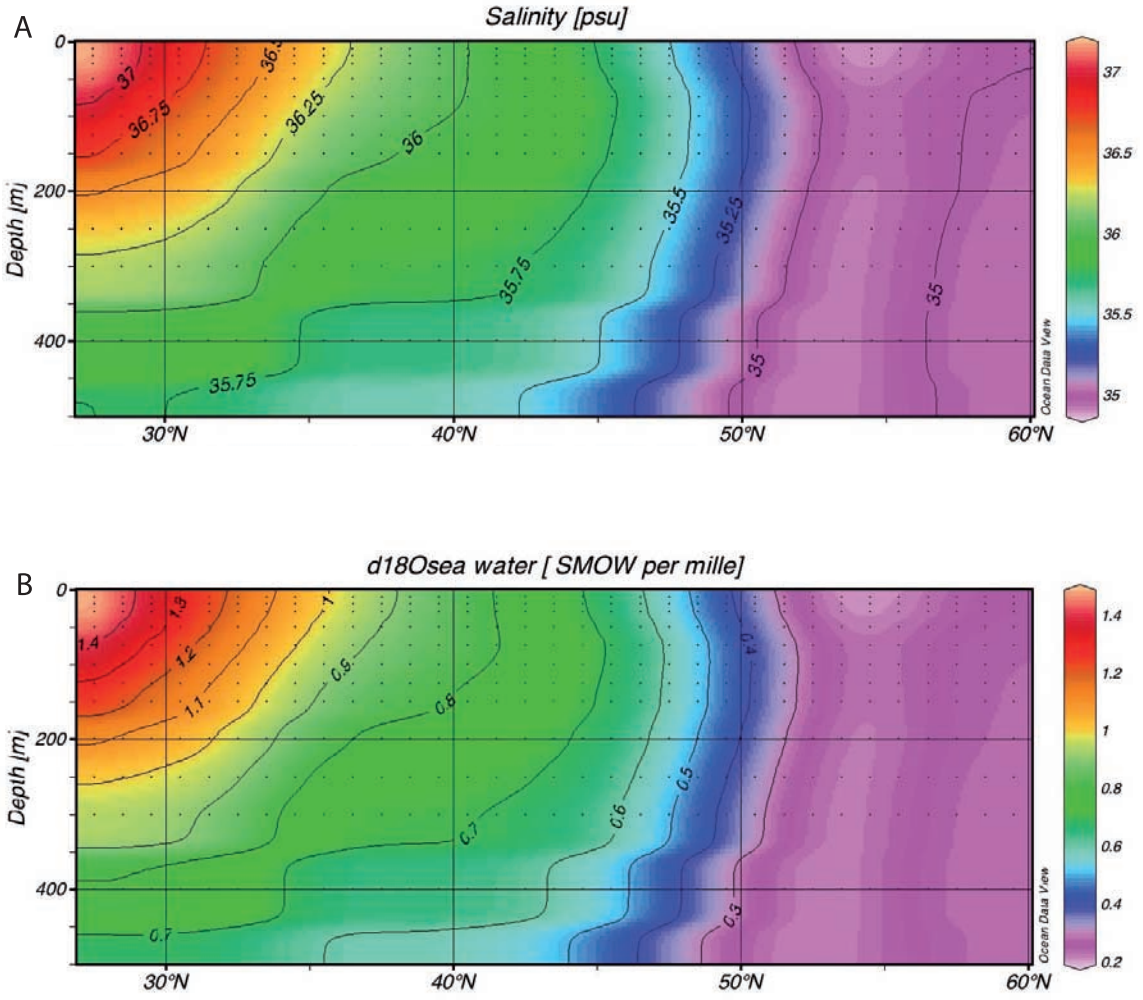

Figure A1. (a) Mean annual salinity and (b) corresponding oxygen isotopic composition of seawater along a 30°W section between 0 and 500 m depth.

Appendix A

[39] Figure A1 shows the decrease of water column stratification from low to high latitudes. North of 45°N, salinity and isotopic composition of seawater are constant through the first five hundred meters. At low latitude, maximum salinity (isotopic composition of seawater) change over this depth is 1.25 psu (0.7‰).

[40] Calcification depth of *G. inflata* in each core top is drawn in Figure A2. When the BST (base of the summer thermocline; see text) is colder than about 16°C, Tiso (isotopic temperature; see text) of *G. inflata* corresponds to the temperature at the BST (Figures A2a to A2u). When the BST is warmer than 16°C, Tiso of *G. inflata* indicates a deeper habitat, in the upper part of the main thermocline (Figures A2v to A2y).

[41] Figure A3 shows the calcification depth of *G. truncatulinoides* dextral and sinistral. They calcify in the lower part of the seasonal thermocline (Figures A3a to A3n) when the BST is colder than about 16°C. But when the BST is warmer than about 16°C, *G. truncatulinoides* lives deeper in the main thermocline (Figures A3o to A3t).

[42] Figure A4 shows that Tiso of *P. obliquiloculata* reflect those at the BST.

[43] Figure A5 shows the good resemblance between reconstructed Holocene summer profiles from Holocene Tiso of *G. ruber* and *G. inflata* and modern temperature profiles extracted from World Ocean Atlas (2001) for the cores along the NW African margin.

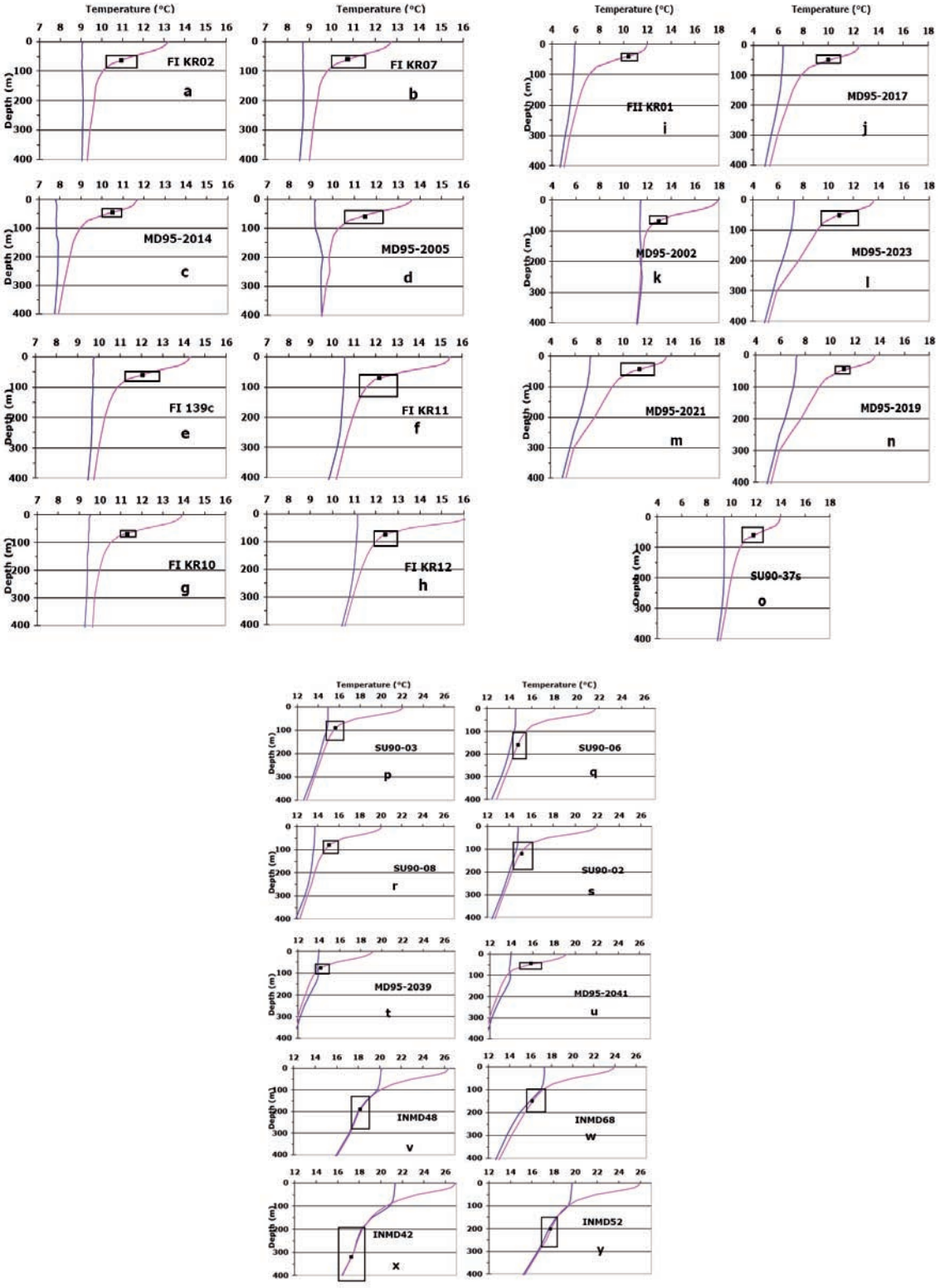

Figure A2. Comparison of the Tiso of *G. inflata* with modern temperatures. Blue (pink) line is the coldest winter (warmest summer) temperature profile from WOA 2001. Square represents the mean Tiso. Rectangle indicates the possible habitat depth according to one sigma range in Tiso resulting from replicate $\delta^{18}O_{foraminifera}$ measurements. (a) FI KR02, (b) FI KR07, (c) MD95-2014, (d) MD95-2005, (e) FI 139c, (f) FI KR11, (g) FI KR10, (h) FI KR12, (i) FII KR01, (j) MD95-2017, (k) MD95-2002, (l) MD95-2023, (m) MD95-2021, (n) MD95-2019, (o) SU90-37s, (p) SU90-03, (q) SU90-06, (r) SU90-08, (s) SU90-02, (t) MD95-2039, (u) MD95-2041, (v) INMD48, (w) INMD68, (x) INMD42, (y) INMD52.

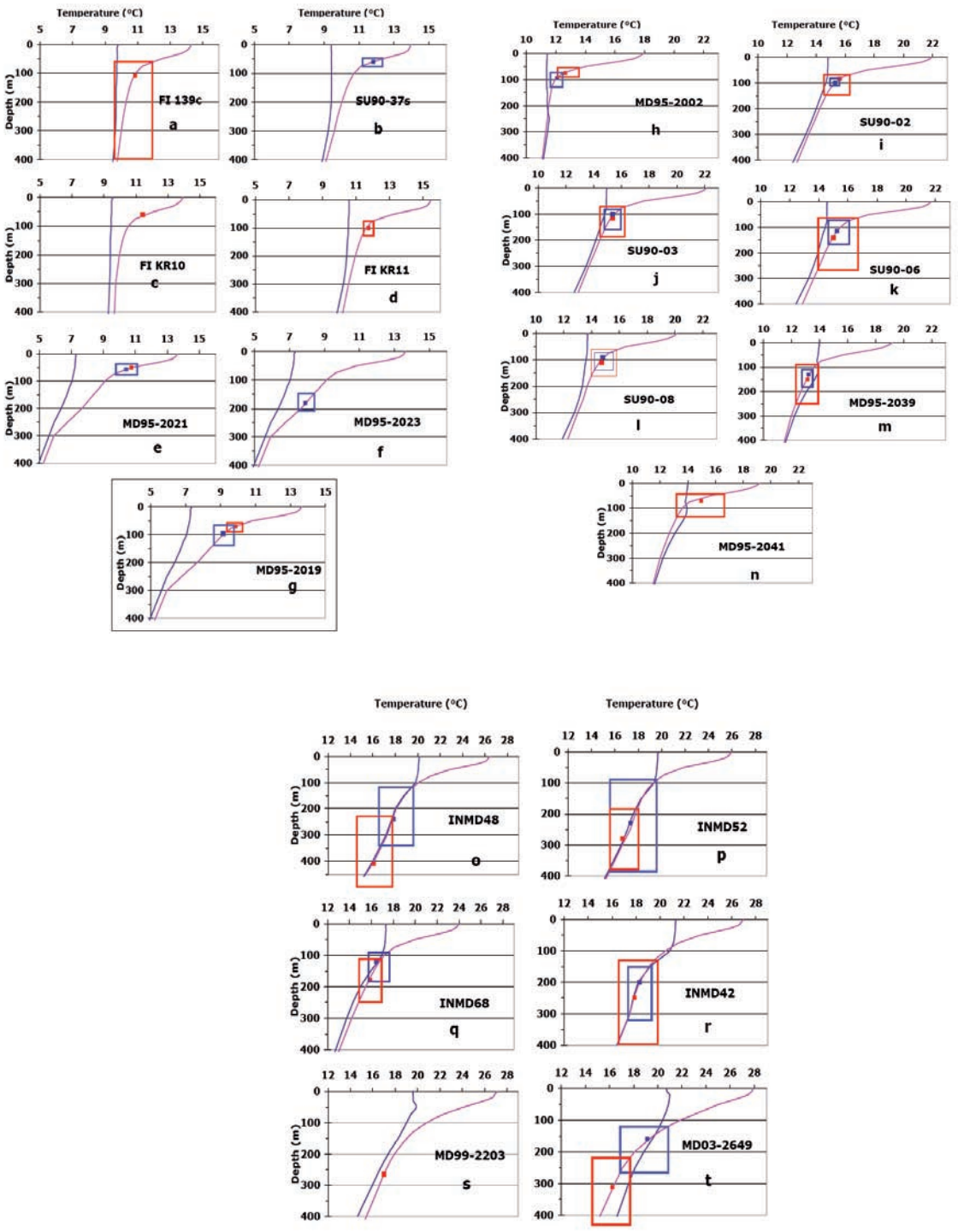

Figure A3. Comparison of Tiso of *G. truncatulinoides* with modern temperatures. Caption same as Figure A2. Red color is used *G. truncatulinoides* dextral data. Blue color is used for *G. truncatulinoides* sinistral data. When only one measurement was made no rectangle was drawn. (a) FI 139C, (b) SU90-37s, (c) FI KR10, (d) FI KR11, (e) MD95-2021, (f) MD95-2023, (g) MD95-2019, (h) MD95-2002, (i) SU90-02, (j) SU90-03, (k) SU90-06, (l) SU90-08, (m) MD95-2039, (n) MD95-2041, (o) INMD48, (p) INMD52, (q) INMD68, (r) INMD42, (s) MD99-2203, (t) MD03-2649.

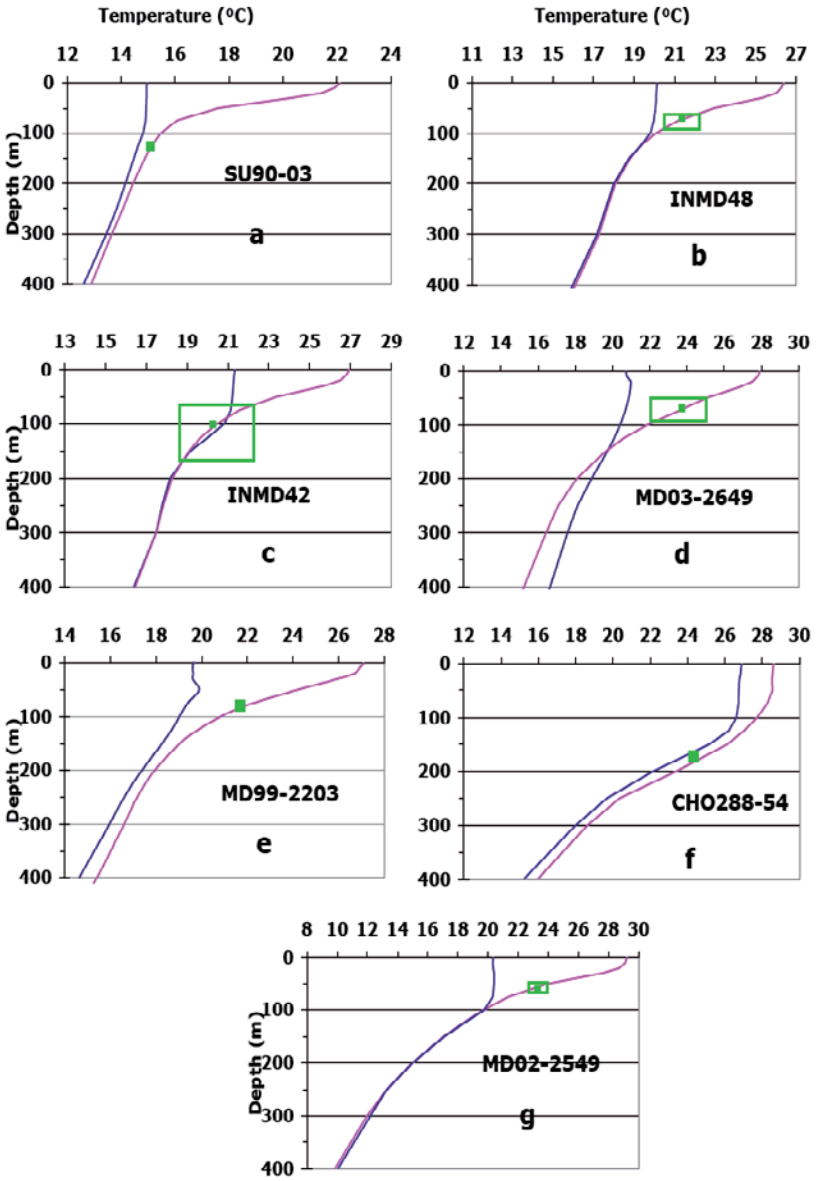

Figure A4. Comparison of Tiso of *P. obliquiloculata* with modern temperatures. Caption same as Figure A2. (a) SU90-06, (b) INMD48, (c) INMD42, (d) MD03-2649, (e) MD99-2203, (f) CHO288-54, (g) MD02-2549.

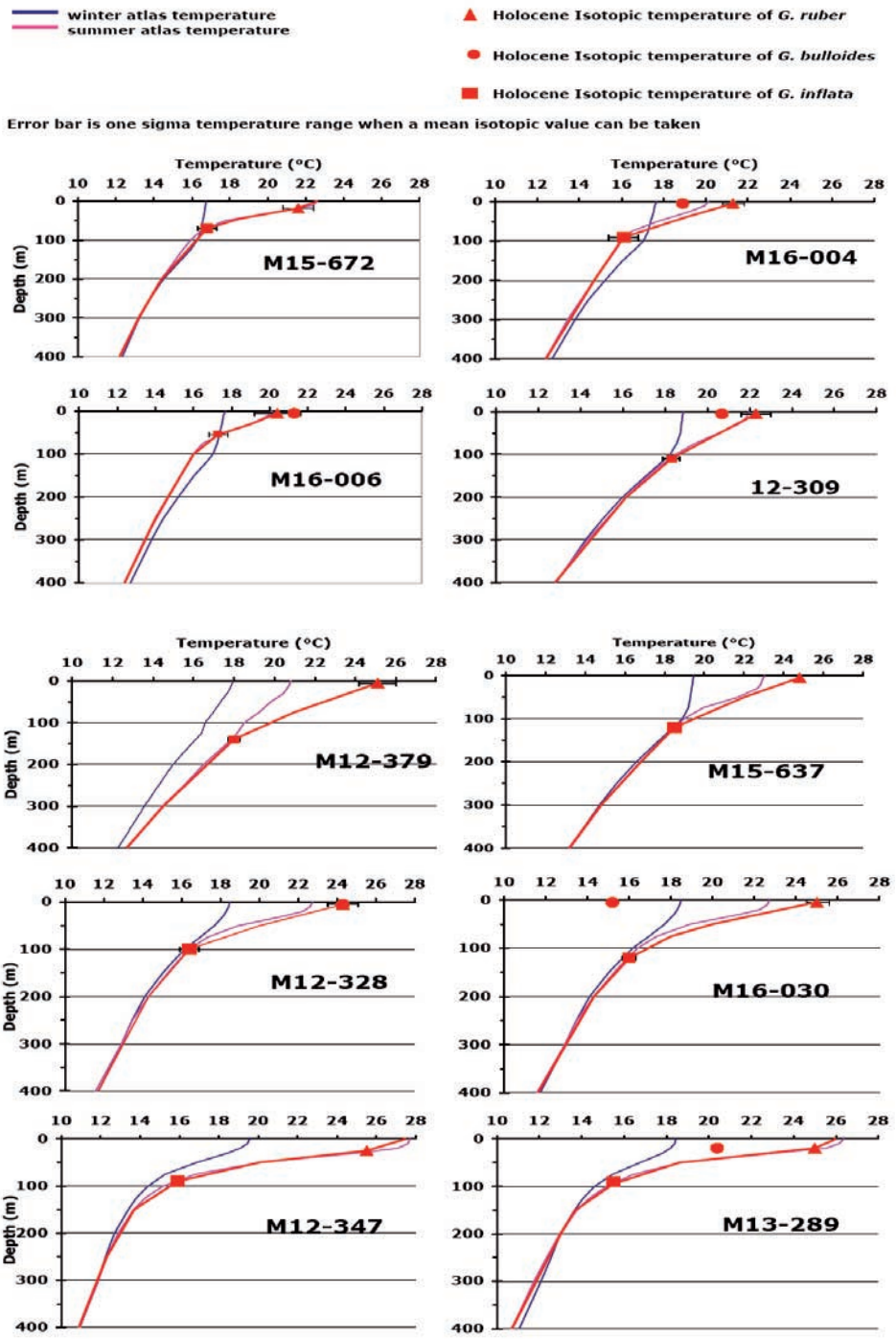

Figure A5. Comparison of Holocene Tiso of *G. ruber*, *G. bulloides* and *G. inflata* with modern temperature profiles for the cores along the NW African margin.

Acknowledgments

[44] The material for the calibration was taken during several oceanographic cruises, noticeably the IMAGES cruises. We thank IFREMER and IPEV for technical support and making the R/V available. We thank the Scripps Institution of Oceanography for providing the INMD samples and J. Duprat (EPOC-Bordeaux) for establishing the stratigraphy of many cores. We thank colleagues of LSCE, C. Waelbroeck, L. Labeyrie, and E. Michel, for careful reading and constructive remarks, and F. Dewilde and B. Le Coat for mass spectrometer analyses. C.C. is supported by a French Research Ministry fellowship. Basic support from CNRS and CEA to LSCE is acknowledged. ANR Forclim and PICC grants provided funds for this study.

References

Bé, A. W. H. (1977), An ecological, zoogeographic and taxonomic review of recent planktonic foraminifera, in *Oceanic Micropaleontology*, vol. 1, edited by A. T. S. E. Ramsay, pp. 1–100, Elsevier, New York.

Bemis, B. E., H. J. Spero, J. Bijma, and D. W. Lea (1998), Reevaluation of the oxygen isotopic composition of planktonic foraminifera: Experimental results and revised paleotemperature equations, *Paleoceanography*, *13*(2), 150–160.

Bertrand, P., et al. (1996), The glacial ocean productivity hypothesis: The importance of regional temporal and spatial studies, *Mar. Geol.*, *130*, 1–9.

Bouvier-Soumagnac, Y., and J.-C. Duplessy (1985), Carbon and oxygen isotopic composition of planktonic foraminifera from laboratory culture, plankton tows and recent sediment: Implications for the reconstruction of paleoclimatic conditions and of the global carbon cycle, *J. Foraminifera Res.*, *15*(4), 302–320.

Colebrook, J. M. (1982), Continuous plankton records: seasonal variations in the distribution and abundance of plankton in the North Atlantic Ocean and the North Sea, *J. Plankton Res.*, *4*, 435–462.

Conkright, M. E., R. A. Locarnini, H. E. Garcia, T. D. O'Brien, T. P. Boyer, C. Stephens, and J. I. Antonov (2002), World Ocean Atlas 2001: Objective Analyses, Data Statistics, and Figures, CD-ROM documentation, *Natl. Oceanogr. Data Cent. Internal Rep. 17*, 17 pp., Silver Spring, Md.

de Vargas, C., S. Renaud, H. Hilbrecht, and J. Pawlowski (2001), Pleistocene adaptive radiation in *Globorotalia truncatulinoides*: Genetic, morphologic, and environmental evidence, *Paleobiology*, *27*(1), 104–125.

Deuser, W. G. (1987), Seasonal variations in isotopic composition and deep-water fluxes of the tests of perennially abundant planktonic foraminifera of the Sargasso Sea: Results from sediment-trap collections and their paleoceanographic significance, *J. Foraminifera Res.*, *17*, 14–27.

Deuser, W. G., and E. H. Ross (1989), Seasonally abundant planktonic foraminifera of the Sargasso Sea—Succession, deep-water fluxes, isotopic composition and paleoceanographic implication, *J. Foraminifera Res.*, *19*, 268–293.

Deuser, W. G., E. H. Ross, C. Hemleben, and M. Spindler (1981), Seasonal changes in species composition, numbers, mass, size, and isotopic composition of planktonic foraminifera settling into the deep Sargasso Sea, *Palaeogeogr. Palaeoclimatol. Palaeoecol.*, *33*, 103–127.

Duplessy, J.-C., L. Labeyrie, A. Juillet-Leclerc, F. Maitre, J. Duprat, and M. Sarnthein (1991), Surface salinity reconstruction of the north Atlantic Ocean during the last glacial maximum, *Oceanol. Acta*, *14*(4), 311–324.

Durazzi, J. T. (1981), Stable-isotope studies of planktonic foraminifera in North Atlantic core tops, *Palaeogeogr. Palaeoclimatol. Palaeoecol.*, *33*, 157–172.

Epstein, S., R. Buchsbaum, H. A. Lowenstam, and H. C. Urey (1953), Revised carbonate-water isotopic temperature scale, *Bull. Geol. Soc. Am.*, *64*, 1315–1326.

Esaias, W. E., G. C. Feldman, C. R. McClain, and J. A. Elrod (1986), Monthly satellite-derived phytoplankton pigment distribution for the North Atlantic Ocean basin, *Eos Trans AGU*, *67*, 835–837.

Fairbanks, R. G., P. H. Wiebe, and A. W. H. Bé (1980), Vertical distribution and isotopic composition of living planktonic foraminifera in the western North Atlantic, *Science*, *207*, 61–63.

Freudenthal, T., H. Meggers, J. Henderiksb, H. Kuhlmanna, A. Moreno, and G. Wefer (2002), Upwelling intensity and filament activity off Morocco during the last 250,000 years, *Deep Sea Res., Part II*, *49*, 3655–3674.

Ganssen, G. (1983), Dokumentation von küstennahem Auftrieb anhand stabiler Isotopen in rezenten Foraminiferen vor Nordwest-Afrika., *Meteor Forschungsergeb., Reihe C*, *37*, 1–46.

Ganssen, G., and D. Kroon (2000), The isotopic signature of planktonic foraminifera from NE Atlantic surface sediments: Implications for the reconstruction of past oceanic conditions, *J. Geol. Soc. London*, *157*, 693–699.

Ganssen, G., and M. Sarnthein (1983), Stable-isotope composition of foraminifers: The surface and bottom water record of coastal upwelling, in *Coastal Upwelling: Its Sediment Record*, Part A, edited by E. Suess and J. Thiede, pp. 99–121, Springer, New York.

Giraudeau, J., M. Cremer, S. Manthé, L. Labeyrie, and G. Bond (2000), Coccolith evidence for instabilities in surface circulation south of Iceland during Holocene times, *Earth Planet. Sci. Lett.*, *179*, 257–268.

Henderiks, J., and J. Bollman (2004), The Gephyrocapsa sea surface palaeothermometer put to the test: Comparison with alkenone and foraminifera proxies off NW Africa, *Mar. Micropaleontol.*, *50*, 161–184.

Hooghiemstra, H., A. Bechler, and H.-J. Beug (1987), Isopollen maps for 18,000 years BP of the Atlantic offshore of North-west Africa: Evidence for paleowind circulation, *Paleoceanography*, *2*, 561–582.

Hull, H., and A. G. Turnbull (1973), A thermochemical study of monohydrocalcite, *Geochim. Cosmochim. Acta*, *37*, 685–694.

Hut, G. (1987), Consultants group meeting on stable isotope reference samples for geochemical and hydrological investigations, Vienna, Austria, 16–18 September 1985, IAEA report, Int. At. Energy Agency, Vienna.

Kim, S. T., and J. R. O'Neil (1997), Equilibrium and nonequilibrium oxygen isotope effects in synthetic carbonates, *Geochim. Cosmochim. Acta*, *61*, 3461–3475.

Koç Karpuz, N., and H. Schrader (1990), Surface sediment diatom distribution and Holocene paleotemperature variations in the Greenland, Iceland and Norwegian Sea, *Paleoceanography*, *5*(4), 557–580.

Kucera, M., A. Rosell-Melé, R. Schneider, C. Waelbroeck, and M. Weinelt (2005), Multiproxy approach for the reconstruction of the glacial ocean surface (MARGO), *Quat. Sci. Rev.*, *24*, 813–819.

LeGrande, A. N., J. Lynch-Stieglitz, and E. C. Farmer (2004), Oxygen isotopic composition of *Globorotalia truncatuli-*

noides as a proxy for intermediate depth density, *Paleoceanography*, *19*, PA4025, doi:10.1029/2004PA001045.

Liu, Z., and S. G. H. Philander (2001), Tropical-extratropical oceanic exchange pathways, in *Ocean Circulation and Climate: Observing and Modeling the Global Ocean*, pp. 247–257, Elsevier, New York.

Martin, P. A., D. W. Lea, Y. Rosenthal, N. J. Shackleton, M. Sarnthein, and T. Papenfuss (2002), Quaternary deep sea temperature histories derived from benthic foraminiferal Mg/Ca, *Earth Planet. Sci. Lett.*, *198*, 193–209.

Martinez, P., P. Bertrand, G. B. Shimmield, K. Cochrane, F. J. Jorissen, J. Foster, and M. Dignan (1999), Upwelling intensity and ocean productivity changes off Cape Blanc (northwest Africa) during the last 70,000 years: Geochemical and micropalaeontological evidence, *Mar. geol.*, *158*, 57–74.

McKenna, V. S., and W. L. Prell (2004), Calibration of the Mg/Ca of *Globorotalia truncatulinoides* (R) for the reconstruction of marine temperature gradients, *Paleoceanography*, *19*, PA2006, doi:10.1029/2000PA000604.

Mortyn, P. G., and C. D. Charles (2003), Planktonic foraminiferal depth habitat and $\delta^{18}O$ calibrations: Plankton tow results from the Atlantic sector of the Southern Ocean, *Paleoceanography*, *18*(2), 1037, doi:10.1029/2001PA000637.

Mulitza, S., A. Dürkoop, W. Hale, G. Wefer, and H. S. Niebler (1997), Planktonic foraminifera as recorders of past surface-water stratification, *Geology*, *25*(4), 335–338.

Mulitza, S., H. W. Arz, Mücke, C. Moos, H. S. Niebler, J. Pätzold, and M. Segl (1999), The south Atlantic carbon isotope record of planktic foraminifera, in *Use of Proxies in Paleoceanography: Examples From the South Atlantic*, edited by G. Fisher and G. Wefer, pp. 427–445, Springer, New York.

Niebler, H. S., H. W. Hubberten, and R. Gersonde (1999), Oxygen isotope values of planktic foraminifera: a tool for the reconstruction of surface water stratification, in *Use of Proxies in Paleoceanography: Examples From the South Atlantic*, edited by G. Fisher and G. Wefer, pp. 165–189, Springer, New York.

Ostermann, D. R., and W. B. Curry (2000), Calibration of stable isotopic data: An enriched $\delta^{18}O$ standard used for source gas mixing detection and correction, *Paleoceanography*, *15*(3), 353–360.

Ottens, J. (1992), April and August northeast Atlantic surface water masses reflected in planktic foraminifera, *Neth. J. Sea Res.*, *28*(4), 261–283.

Prell, W. L. (1985), The stability of low-latitude sea-surface temperatures: An evaluation of the CLIMAP reconstruction with emphasis on the positive SST anomalies, U. S. Dept. of Energy, Washington, D. C.

Ravelo, A. C., and R. G. Fairbanks (1990), Reconstructing tropical Atlantic hydrography using planktonic foraminifera and an ocean model, *Paleoceanography*, *5*(3), 409–431.

Ravelo, A. C., and R. G. Fairbanks (1992), Oxygen isotopic composition of multiple species of planktonic foraminifera: Recorders of the modern photic zone temperature gradient, *Paleoceanography*, *7*(6), 815–831.

Sarmiento, J. L., N. Gruber, M. A. Brzezinski, and J. P. Dunne (2004), High-latitude controls of the thermocline nutrients and low latitude biological productivity, *Nature*, *427*, 56–60.

Sarnthein, M., K. Winn, S. Jung, J.-C. Duplessy, L. Labeyrie, H. Erlenkeuser, and G. Ganssen (1994), Changes in east Atlantic deepwater circulation over the last 30,000 years: Eight time slice reconstructions, *Paleoceanography*, *9*(6), 209–267.

Schrag, D. P., and B. K. Linsley (2002), Corals, chemistry, and climate, *Science*, *296*, 277–278.

Shackleton, N. J. (1974), Attainment of isotopic equilibrium between ocean water and benthonic foraminifera genus Uvigerina: isotopic changes in the ocean during the last glacial, in *Les Méthodes Quantitatives d'Etude des Variations du Climat au Cours du Pleistocène*, pp. 203–209, Cent. Natl. de la Rech. Sci., Gif sur Yvette, France.

Streeter, S. S., and N. J. Shackleton (1979), Paleocirculation of the deep North Atlantic: 150,000-year record of benthic foraminifera and oxygen-18, *Science*, *203*, 168–170.

Wang, L., M. Sarnthein, J.-C. Duplessy, H. Erlenkeuser, S. Jung, and U. Pflaumann (1995), Paleo sea surface salinities in the low-latitude Atlantic: The $\delta^{18}O$ record of *Globigerinoides ruber* (white), *Paleoceanography*, *10*(4), 749–761.

Wilke, I., T. Bickert, and F. J. C. Peeters (2006), The influence of seawater carbonate ion concentration [CO_3^{2-}] on the stable carbon isotope composition of the planktic foraminifera species *Globorotalia inflata*, *Mar. Micropaleontol.*, *58*, 243–258.

Zahn, R. (1986), Spätquartäre Entwicklung von Küstenauftrieb und Tiefenwasserzirkulation in Nordost-Atlantik. Rekonstruktion anhand stabiler Isotope kalkschaliger Foraminiferen, Ph.D. thesis, Univ. of Kiel, Kiel, Germany.

Zahn, R., and M. Sarnthein (1987), Benthic isotope evidence for changes of the Mediterranean outflow during the late quaternary, *Paleoceanography*, *2*(6), 543–559.